A&A 541, A66 (2012)
DOI: 10.1051/0004-6361/201118489

Astronomy & Astrophysics

Spectral monitoring of RX J1856.5-3754 with *XMM-Newton*

Analysis of EPIC-pn data

N. Sartore[1], A. Tiengo[1,2], S. Mereghetti[1], A. De Luca[1,2,3], R. Turolla[4,5], and F. Haberl[6]

[1] INAF – Istituto di Fisica Spaziale e Fisica Cosmica, via E. Bassini 15, 20133 Milano, Italy
e-mail: sartore@iasf-milano.inaf.it
[2] IUSS – Istituto Universitario di Studi Superiori, viale Lungo Ticino Sforza 56, 27100 Pavia, Italy
[3] INFN – Istituto Nazionale di Fisica Nucleare, sezione di Pavia, via A. Bassi 6, 27100 Pavia, Italy
[4] Dipartimento di Fisica e Astronomia, Università di Padova, via Marzolo 8, 35131 Padova, Italy
[5] Mullard Space Science Laboratory, University College London, Holmbury St. Mary, Dorking, Surrey, RH5 6NT, UK
[6] Max-Planck-Institut für extraterrestrische Physik, Giessenbachstraße, 85748 Garching bei München, Germany

Received 20 November 2011 / Accepted 8 February 2012

ABSTRACT

Using a large set of *XMM-Newton* observations, we searched for the long-term spectral and flux variability of the isolated neutron star RX J1856.5-3754 in the time interval from April 2002 to October 2011. This is the brightest and most extensively observed source of a small group of nearby, thermally emitting isolated neutron stars, of which at least one member (RX J0720.4-3125) has shown long-term variability. A detailed analysis of the data obtained with the EPIC-pn camera in the 0.15−1.2 keV energy range reveals only small variations in the temperature derived with a single blackbody fit (of about 1% around an average value of $kT^{\infty} \sim 61$ eV). These variations appear to be correlated with the position of the source on the detector and can be ascribed to an instrumental effect, most likely a spatial dependence of the channel-to-energy relation. For the sampled instrumental coordinates, we quantify this effect as variations of ∼4% and ∼15 eV in the gain slope and offset, respectively. Selecting only a homogeneous subset of observations, with the source imaged at the same detector position, we find no evidence of either spectral or flux variations of RX J1856.5-3754 from March 2005 to the present-day, with limits of $\Delta kT^{\infty} < 0.5\%$ and $\Delta f_{\rm X} < 3\%$ (0.15−1.2 keV range), with 3σ confidence. A slightly higher temperature ($kT^{\infty} \sim 61.5$ eV, compared to the average value of $kT^{\infty} \sim 61$ eV) was instead measured in April 2002. If this difference is not of instrumental origin, it implies a rate of variation ∼–0.15 eV yr^{-1} between April 2002 and March 2005. The high-quality-statistics source spectrum from the selected observations is best fitted with the sum of two blackbody models, with temperatures of $kT_{\rm h}^{\infty} = 62.4^{+0.6}_{-0.4}$ eV and $kT_{\rm s}^{\infty} = 38.9^{+4.9}_{-2.9}$ eV, which can also account for the flux seen in the optical band. No significant narrow or broad spectral features are detected, with upper limits of ∼6 eV on their equivalent width.

Key words. stars: neutron – X-rays: stars – stars: individual: RX J1856.5-3754

1. Introduction

RX J1856.5-3754 (J1856 hereafter) is the prototype of the so-called XDINSs, i.e. the seven X-ray dim isolated neutron stars discovered by the ROSAT satellite (e.g. Walter et al. 1996; see also Haberl 2007; Turolla 2009, for reviews). These are nearby, $d \lesssim 300$ pc, radio-quiet isolated neutron stars characterized by thermal spectra, with temperatures[1] $kT^{\infty} \sim 50-100$ eV and luminosities $L_{\rm X} \sim 10^{31}-10^{32}$ erg s^{-1}. Six out of the seven XDINSs exhibit broad spectral features at energies between 270 eV and 700 eV, with equivalent widths of several tens of eV, interpreted as proton cyclotron lines or atomic transitions in strong magnetic fields, $B \sim 10^{13}$ G. The spin periods of the XDINSs are in the 3–12 s range and, assuming magneto-dipole braking, their measured spin-down rates, of $\sim 10^{-14}-10^{-13}$ s s^{-1}, imply magnetic fields $B \sim 10^{13}-10^{14}$ G, in broad agreement with those inferred from the spectral features. All XDINSs have very faint optical/UV counterparts, $m_V \sim 26-27$ but the optical/UV flux exceeds that expected from the Rayleigh-Jeans tail of the X-ray blackbody (BB, see e.g. Kaplan et al. 2011).

Intriguingly, the second brightest XDINS, RX J0720.4-3125 (J0720 hereafter) has displayed significant long-term variations in its spectral properties (Hohle et al. 2010, and references therein). The nature of these changes is still under debate and can possibly be related to either a precession of its spin axis (e.g. Haberl et al. 2006) or a glitch-like episode (van Kerkwijk et al. 2007). Another interesting result is that XDINSs share some of their properties with magnetars. In particular, their spin periods fall in the same range, while the magnetic fields of XDINSs are in-between those of magnetars, $B \sim 10^{14}-10^{15}$ G, and normal pulsars, $B \sim 10^{11}-10^{13}$ G. In addition, XDINSs seem to be older than magnetars, with spindown ages of $\sim 10^5-10^6$ years compared to $\sim 10^3-10^5$ years for magnetars (e.g. Mereghetti 2008). These similarities suggest that there is an evolutionary link between the two classes of isolated neutron stars (INSs).

Among known XDINSs, J1856 has the lowest pulsed fraction, ∼1% (Tiengo & Mereghetti 2007), and the weakest magnetic field, $B \sim 1.5 \times 10^{13}$ G (van Kerkwijk & Kaplan 2008). Being the brightest, $f_{\rm X} \sim 1.5 \times 10^{-11}$ erg s^{-1} cm^{-2}, and closest of the category, $d = 123^{+11}_{-15}$ pc (e.g. Walter et al. 2010), it is among the best candidates to probe the mass and radius of a neutron star, which in turn would be of paramount importance to constrain the equation of state (EOS) of matter at nuclear densities. Analyzing the data from a 57 ks *XMM-Newton* observation and a ∼500 ks observation by *Chandra*, Burwitz et al. (2003)

[1] As measured by an observer at infinity.

Table 1. Log of all EPIC-pn observations of RX J1856.5-3754 performed in small window mode.

Observation	Date	Obs. ID	Net exposure time [s]	Counts
A	2002-04-08	0106260101	40 030	302601
B	2004-09-24	0165971601	22 960	174955
C	2005-03-23	0165971901	14 190	106949
D	2005-09-24	0165972001	22 700	168609
E	2006-03-26	0165972101	48 340	361845
F	2006-10-24	0412600101	49 820	374018
G	2007-03-14	0412600201	26 940	204513
H	2007-03-25	0415180101	16 540	126883
I	2007-10-04	0412600301	23 920	179449
J	2008-03-13	0412600401	33 080	245923
K	2008-10-04	0412600601	43 580	330553
L	2009-03-19	0412600701	47 510	353698
M	2009-10-07	0412600801	40 780	306449
N	2010-03-22	0412600901	48 380	360306
O	2010-09-29	0412601101	47 870	356580
P	2011-03-14	0412601301	45 210	342204
Q1	2011-10-05*	0412601501	17 490	134747
Q2	”	”	16 310	124431
Q2	”	”	16 800	127176
Q4	”	”	17 920	128549

Notes. (*) The observation of October 2011 has been divided in four pointings, with the source at different positions on the detector.

suggested that atmospheric models with heavy elements can be ruled out, given the lack of any spectral features. In addition, they ruled out non-magnetic and fully ionized hydrogen atmosphere models, since both would overpredict the optical flux. On the other hand, they found that the broadband (optical + X-ray) spectrum is well-fitted by a two-component BB, where the hotter component, $kT_{\rm X}^{\infty} \simeq 63.5$ eV ($R_{\rm X}^{\infty} \simeq 4.4\,(d/120\,{\rm pc})$ km) is responsible for the X-ray emission, while the cold component, $kT_{\rm opt} < 33$ eV ($R_{\rm opt}^{\infty} > 17\,(d/120\,{\rm pc})$ km), accounts only for the optical emission. Alternative models, such as emission from condensed matter surface (Lai 2001; Turolla et al. 2004), or partially ionized hydrogen atmospheres (Ho et al. 2007) cannot be ruled out.

Thanks to its bright and presumably steady emission, J1856 has been targeted routinely for calibration purposes by *XMM-Newton* in the past decade. The large amount of collected data allows us to precisely characterize its spectral evolution on timescales from months to ∼10 years. At the same time, the stability of the detectors onboard *XMM-Newton* in the same timeframe can also be scrutinized, as done with the data taken before 2006 in Haberl (2007). Here we report on the analysis of all *XMM-Newton* observations of J1856 performed so far in imaging mode with the EPIC-pn camera (Strüder et al. 2001) onboard *XMM-Newton*. The reduction and the analysis of the data is described in Sect. 2. Results are also illustrated in Sect. 2. We constrain the detector stability and obtain an upper limit to the spectral variations of the star, which we then compare to those of other isolated neutron stars reported in the literature. A discussion on the astrophysical implications of these results is also given (Sect. 3). We draw our conclusions in Sect. 4.

2. Data reduction and spectral analysis

We use all imaging data collected with the EPIC-pn camera from April 2002 to October 2011. Data from the two EPIC-MOS detectors are not considered in this analysis because the MOS effective area at soft X-ray energies is much smaller than that of the pn and the MOS cameras are known to be less stable in the long term (Read et al. 2006). Table 1 reports the date, identification number, net exposure time, and number of background-subtracted counts of J1856 for each observation. All observations were performed in small window mode with the thin filter. Raw data are processed with the *XMM-Newton* science analysis package (SAS) v11.0, using the `epproc` pipeline. We then build light curves above 10 keV, with bin size of 100 s, in order to identify soft proton flares. On the basis of these light curves, we clean the data by removing time intervals with count rates higher than 4σ above the mean rate. Source spectra are then extracted from a circular region of 30″ radius, selecting only single pixel events (i.e. PATTERN = 0 in the `xmmselect` task), to obtain event lists of the highest possible quality. The extracted spectra are binned in order to have at least 30 counts per bin. The spectral analysis is performed with XSPEC 12 (Arnaud 1996), selecting photon energies in the 0.15−1.2 keV range.

We perform a simultaneous fit of all the 20 spectra with a single absorbed BB, using a `phabs*bbodyrad` model and adopting the abundances of Anders & Grevesse (1989). The true spectra of XDINSs can be more complex than a single BB. However, we are interested in relative variations in the emission of J1856. Thus, we rely on the parameters of the single BB in order to quantify these variations. The best fit gives a BB temperature $kT^{\infty} = 61.30 \pm 0.04$ eV, and a column density $N_{\rm H} = (5.84 \pm 0.04) \times 10^{19}\,{\rm cm}^{-2}$ ($\chi^2_\nu = 1.78$ with 2784 degrees of freedom). The residuals show large systematic deviations, especially above ∼0.5 keV (Fig. 1, upper panel), which change from observation to observation, indicating that some of the spectral parameters vary between different observations. Therefore, we repeat the spectral fit leaving the BB temperature and normalization as free parameters for each observation. In this case, we obtain a better $\chi^2_\nu = 1.37$ with 2746 degrees of freedom. The resulting parameters are shown in Fig. 2 (panels *a*, *b*, *c*). The fit of the 20 spectra in which the column density is free parameter, and there is a unique temperature and normalization for all observations, is not as good as the previous one, $\chi^2_\nu = 1.58$

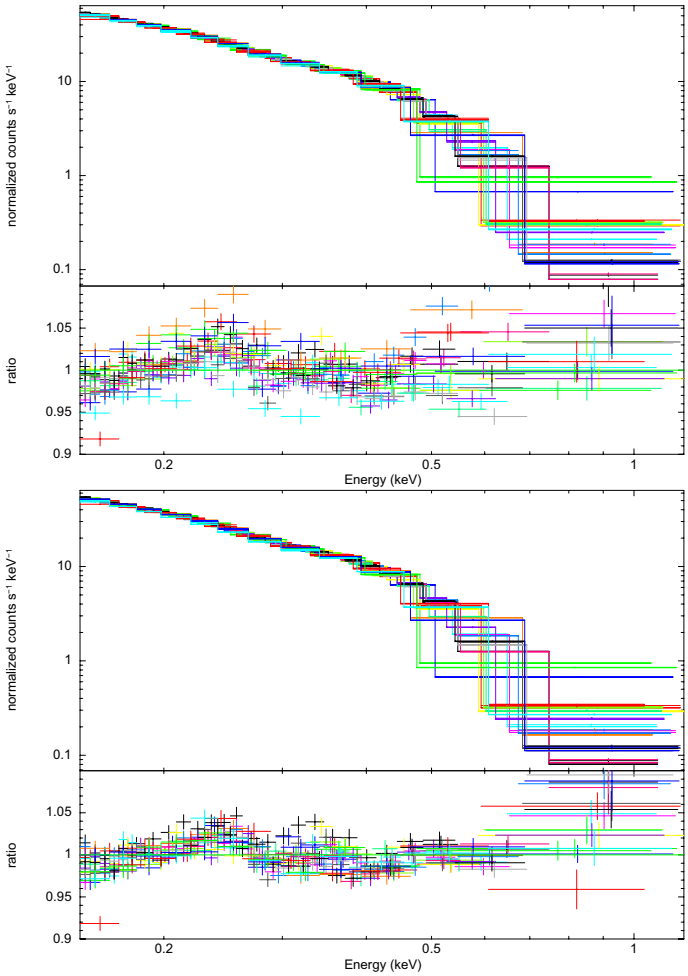

Fig. 1. Simultaneous fit of all J1856 spectra with the same single BB. *Upper (lower) panel* shows the residuals without (with) any freedom in the gain parameters during fitting.

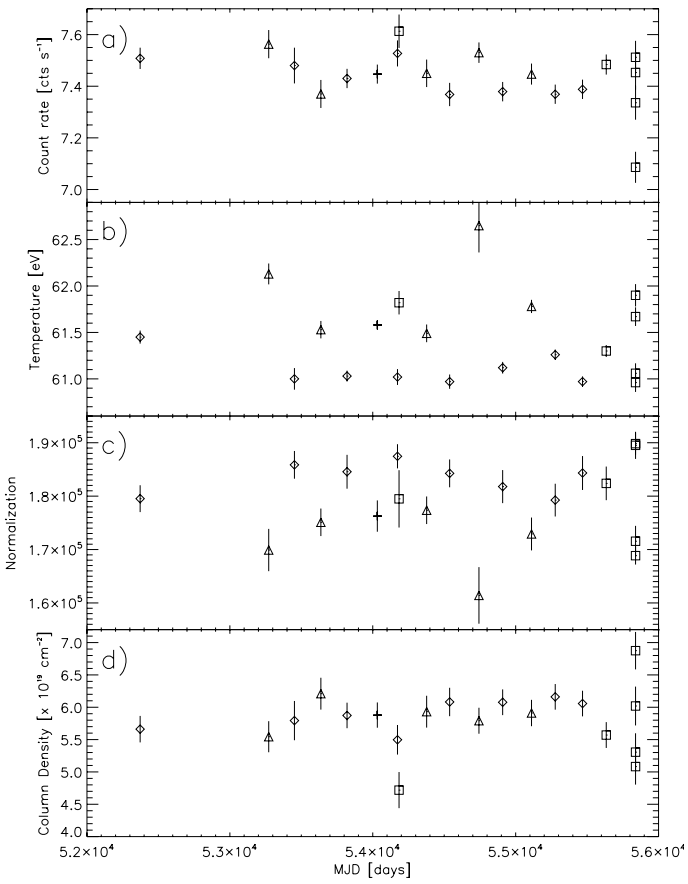

Fig. 2. Long-term evolution of the spectral parameters obtained with a single BB fit in the 0.15−1.2 keV range. Panels **a)**, **b)**, and **c)**, show the count rate, temperature, and BB normalization of a simultaneous fit with the column density fixed to a common value. Panel **d)** indicates the column density obtained when, instead, the BB parameters are fixed to a common value for all the observations (see text). Diamonds, triangles, and squares represent "soft", "hard", and off-axis observations, respectively. The plus symbol is the October 2006 observation, which is at an intermediate detector position (see Fig. 3). Error bars correspond to 3σ confidence intervals.

with 2765 degrees of freedom. The resulting column densities are shown in Fig. 2 (panel *d*). The count rate shows variations of ∼1−2 percent around a mean of ∼7.46 cts s^{-1}, but there is no evidence of a defined trend nor any correlation with either the BB temperature or normalization. On the other hand, the hydrogen column density is clearly anti-correlated with the count rate (compare panels *a* and *d* in Fig. 2), indicating that the changes in the count rate are mainly determined by differences in the softest spectral band. As already noticed by Stuhlinger et al. (2010), the temperature also has variations of ∼1−2 percent (∼1.5−2 eV), which are anti-correlated with the normalization. We note that these variations have a seasonal pattern with a period of ∼12 months, suggesting that they are likely related to instrumental effects rather than being intrinsic changes in the source emission. To verify this hypothesis, we study the relation between the BB temperature with the position of the source centroid on the detector (RAWX and RAWY coordinates). With the exception of the three off-axis observations (observations H, P, and Q, which includes the four separate pointings performed in October 2011) and one in an intermediate position (observation F), in most of the observations the source centroid lies in two close but distinct regions of the detector (Fig. 3), one at RAWX ∼ 36−37, RAWY ∼ 192, and the other one at RAWX ∼ 38, RAWY ∼ 190 (hereafter the "soft" and "hard" region, respectively, according to the relative hardness of their spectra, as outlined below). This is due to the different roll angle of the satellite in the spring and fall visibility intervals for the J1856 sky region.

The best-fit BB temperature is systematically higher for observations with the source in the "hard" region (upper right and lower left panels of Fig. 3), and in the three most extreme off-axis observations at RAWY = 168, RAWX = 16, and RAWX = 56. In the pn camera, the signal is read independently from each column along the RAWY position. This implies that small inaccuracies in either the gain or the charge transfer inefficiency (CTI) correction along the readout direction could be the underlying cause of the observed spectral differences. Thus, we fit again all the spectra with a unique BB model, but this time allowing a variation in the gain parameters. These parameters, *slope* and *offset*, define the relation between the energy scale in the response matrix of each observation with respect to that of an observation taken as reference, in order to have $E'_i = E/slope_i - offset_i$. We assume the spectrum of the first observation (observation A) as reference, i.e. we fix its *slope* and *offset* to 1 and 0, respectively. In this case, we obtain $\chi^2_\nu = 1.32$ with 2746 degrees of freedom, with a net reduction in the scatter of the fit residuals for all spectra (Fig. 1, lower panel) and values of the gain parameters ranging from ∼0.986 to ∼1.028 for the *slope* and from ∼−6.6 eV

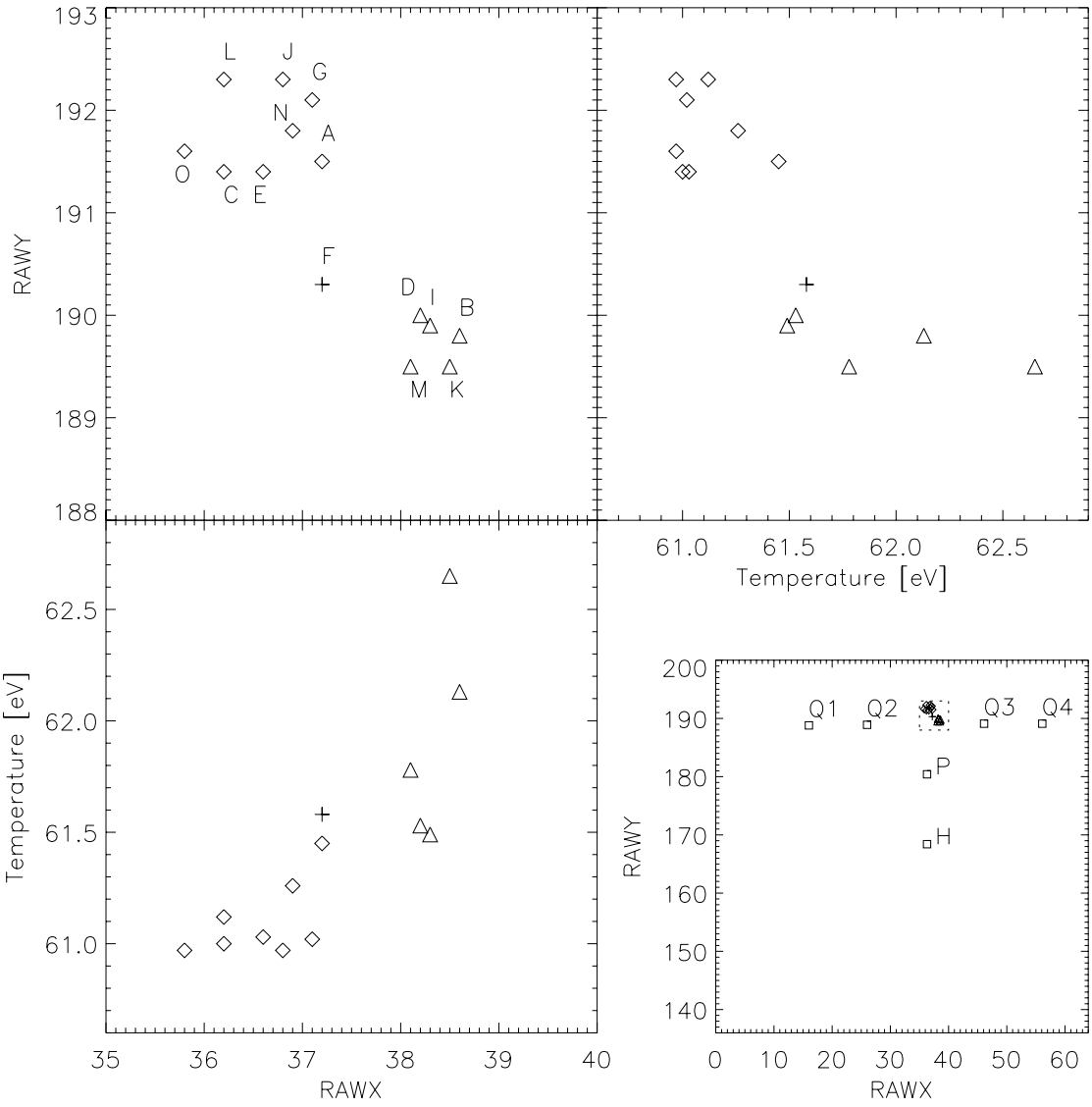

Fig. 3. *Lower right panel*: position of the source in detector coordinates (RAWX, RAWY). The region in the dashed square is enlarged in the *upper left panel*. The symbols indicate the different observations: "soft" region (diamonds), "hard" region (triangles), observation F (plus), and off-axis observations (squares). The other two panels indicate the temperature as a function of the source position.

to ~8.1 eV for the *offset*. This implies that there could be variations of up to ~4% in the *slope* and of ~15 eV in the *offset*[2] throughout the past ten years and source positions sampled by the *XMM-Newton* observations (see Fig. 3). This is a conservative estimate since we considered the two most extreme spectra and assumed no intrinsic spectral variability in J1856.

2.1. Constraints on intrinsic spectral variations

To investigate possible variations in the spectral properties of J1856 during the nine year-long time-span of the monitoring campaign, we have to compare only homogeneous data sets, i.e. when the source was located at approximately the same detector coordinates, to reduce the incidence of the systematic uncertainty reported in the previous section.

We first study temperature variations considering the eight spectra of the observations with the source in the "soft" region. Fitting a linear function to the derived temperatures, we obtain a negative (cooling) rate of variation of $\sim -0.035 \pm 0.010$ eV yr^{-1} (Fig. 4). However, the fit is unacceptable ($\chi^2_\nu = 5.16$ for 6 degrees of freedom) because of the first data point (observation A), which differs significantly from the others. Assuming no variations in the instrument response between April 2002 and March 2005, the "anomalous" temperature inferred from the older spectrum may be explained by an intrinsic change in the source emission, similar to those observed in J0720, implying that there has been a relatively rapid drop in the temperature, of ~0.5 eV in less than three years. Alternatively, some subtle variations in the instrument (energy response of the pixel column) may have occurred in the same time-frame. Excluding the first data point, we obtain a better fit ($\chi^2_\nu = 1.74$ for five

[2] Note that the pn channel energy has a width of ~5 eV, which means that the photon energy as detected by the instrument is not known to any greater certainty than this.

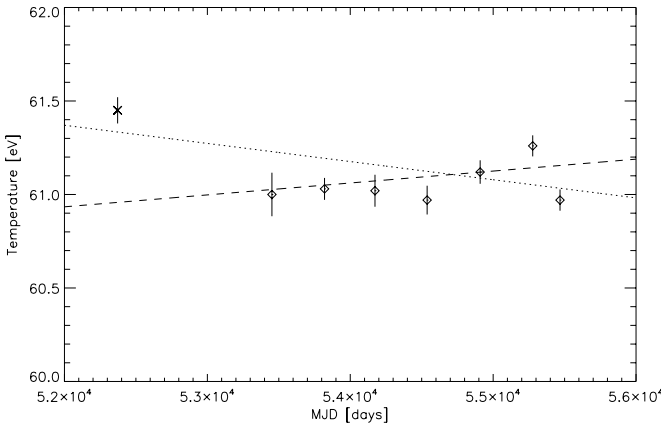

Fig. 4. Long-term evolution of the temperature for "soft" observations. The dotted line represents the linear fit to the data. The dashed line represents a linear fit to the data without considering the observation of April 2002, which is marked by the X symbol. Error bars correspond to 3σ confidence intervals.

degrees of freedom) and the rate of temperature variations of $\sim 0.023 \pm 0.015$ eV yr^{-1}, which is *de facto* consistent with a constant temperature at the 2σ level (Fig. 4).

If instead we use the data from the five "hard" observations, we obtain a rate of temperature variation of $\sim 0.044 \pm 0.026$ eV yr^{-1}, which is again consistent with a constant temperature at 2σ level. However, the value obtained is affected by a larger uncertainty since, as can be seen from the middle panel of Fig. 2, in this case there is a larger scatter in the kT^{∞} values with respect to those found for the "soft" observations. The origin of this larger scatter is unclear and could be possibly related to a gain instability of the pixel columns within the source point spread function. In any case, owing to their homogeneity and longer total exposure, throughout the rest of the paper we make use of only the "soft" data to constrain the spectral properties of J1856.

2.2. Beyond the single blackbody

To obtain a single spectrum with large statistics, we merge together the seven spectra of the "soft" group (Fig. 3) excluding, as before, the anomalous observation of April 2002 (observation A). The resulting spectrum contains $\sim 1.9 \times 10^6$ background-subtracted counts and corresponds to a net integration time of ~254 ks.

We first try fits with a single BB (Fig. 5, upper panel). To obtain a formally acceptable fit (null hypothesis probability > 0.1), we add a systematic error of 1.5% (*systematic* parameter in XSPEC). This is an energy-independent systematic error added to the model in XSPEC and accounts for the uncertainties in the spectral model and for likely residual calibration inaccuracies. We obtain a reduced $\chi^2_\nu = 1.12$ for 176 degrees of freedom. The resulting temperature is $kT^{\infty} = 61.5 \pm 0.1$ eV, which corresponds to an emission radius $R^{\infty} = 5.0 \pm 0.1$ km for a distance of 120 pc. The column density is $N_{\rm H} = (4.8 \pm 0.2) \times 10^{19}$ cm^{-2}. The fit residuals exhibit systematic deviations at both the lowest and highest ends of the energy range (Fig. 5, upper panel), which may be indicative of the inability of the single temperature BB to adequately fit the spectrum of J1856.

The presence of a second BB at a different temperature is expected to explain pulsations (e.g. Tiengo & Mereghetti 2007). We therefore fit the merged spectrum with a two BB model (Fig. 5, lower panel). In this case, we obtain an acceptable fit by adding a systematic error of 0.6%, which returns a $\chi^2_\nu = 1.11$. The column density is now $N_{\rm H} = (12.9 \pm 2.2) \times 10^{19}$ cm^{-2}. The hard BB has a temperature of $kT^{\infty}_{\rm h} = 62.4^{+0.6}_{-0.4}$ eV with emission radius of $R^{\infty}_{\rm h} = 4.7^{+0.2}_{-0.3}\,(d/120\,{\rm pc})$ km, while the soft BB has a temperature $kT^{\infty}_{\rm s} = 38.9^{+4.9}_{-2.9}$ eV and emission radius $R^{\infty}_{\rm s} = 11.8^{+5.0}_{-0.4}\,(d/120\,{\rm pc})$ km. We summarize these results in Table 2. Interestingly, the contribution of both the soft and hard X-ray BBs to the optical flux can account for the excess observed in J1856 (van Kerkwijk & Kulkarni 2001; Kaplan et al. 2011). When considering the best-fit parameters for the double BB model, the contribution of the soft BB at optical wavelengths is about four times larger than that of the hard BB. This implies that at optical wavelengths the flux is of about five times higher than the optical flux expected from the Rayleigh-Jeans tail of the hard BB alone (Fig. 6). This value is consistent, within the uncertainties, to the factor of about seven obtained from the comparison between optical/UV photometry and the extrapolation of the X-ray data (Burwitz et al. 2003; Kaplan et al. 2011).

We note three dips at ~0.3, 0.4, and 0.6 keV in the residuals of both the single and two-component BB fits. Since their width is smaller than the energy resolution of the pn detector in the range of interest, they are most likely due to imperfect instrumental calibrations, as already suggested by Haberl (2007). We search for other possible features in the spectrum of J1856, adopting the single BB model with no systematic errors in order to facilitate the comparison with the spectral features found in other XDINS. We investigate the presence of narrow absorption features from 300 eV to 700 eV at 100 eV intervals. We use the `Gaussian` model from the XSPEC library, imposing a fixed line energy and width[3] ($\sigma = 0$ in XSPEC) and negative normalization. We find a feature at 400 eV, which is most likely one of the aforementioned dips and is therefore of instrumental origin, with equivalent width of 2.0 ± 0.5 eV at 4σ confidence. No other narrow features are found at the same confidence level, for a maximum equivalent width of ~6 eV. Typically, XDINSs exhibit broad absorption lines. Hence, we search for broad features (fixed line-width $\sigma = 0.1$ keV) but allow the line energy to vary. We find a feature at 370 ± 15 eV and equivalent width 9 ± 2 eV at 4σ confidence. However, the reality of this line is debatable and could arise from an attempt to fit a non purely Planckian spectral continuum. If we indeed adopt the two-component BB as a starting model, no broad features are found at the 4σ confidence level.

3. Discussion

Our spectral analysis of all the imaging observations of the isolated neutron star RX J1856.5-3754, performed from 2002 to 2011 with the EPIC-pn instrument onboard the *XMM-Newton* satellite, has revealed small amplitude variations, of about 1–2%, which ca be quantified by changes in the fit parameters obtained with a single absorbed BB model. The long-term trend of these variations has suggested an instrumental origin, since there is a correlation between the fit parameters and the position of the source image on the detector. This is likely related to a non-uniform energy response between different channels of the readout electronics. The related uncertainty has been quantified with a gain fit in XSPEC, resulting in variations of the gain *slope*

[3] The condition $\sigma = 0$ implies that the line width is smaller than the energy resolution. The width σ is thus automatically adjusted to match the minimum width imposed by the instrument resolution.

Table 2. Summary of fit parameters for the combined spectrum.

Parameter	Single BB	Two BB
$N_{\rm H}$ [10^{19} cm^{-2}]	$4.8^{+0.2}_{-0.2}$	$12.9^{+2.2}_{-2.3}$
$kT_{\rm h}^{\infty}$ [eV]	$61.5^{+0.1}_{-0.1}$	$62.4^{+0.6}_{-0.4}$
$R_{\rm h}^{\infty}$ [km]	$5.0^{+0.1}_{-0.1}$	$4.7^{+0.2}_{-0.3}$
$kT_{\rm s}^{\infty}$ [eV]	-	$38.9^{+4.9}_{-2.9}$
$R_{\rm s}^{\infty}$ [km]	-	$11.8^{+5.0}_{-0.4}$
$\sigma_{\rm sys}$	1.5%	0.6%
χ^2_ν	1.12	1.11

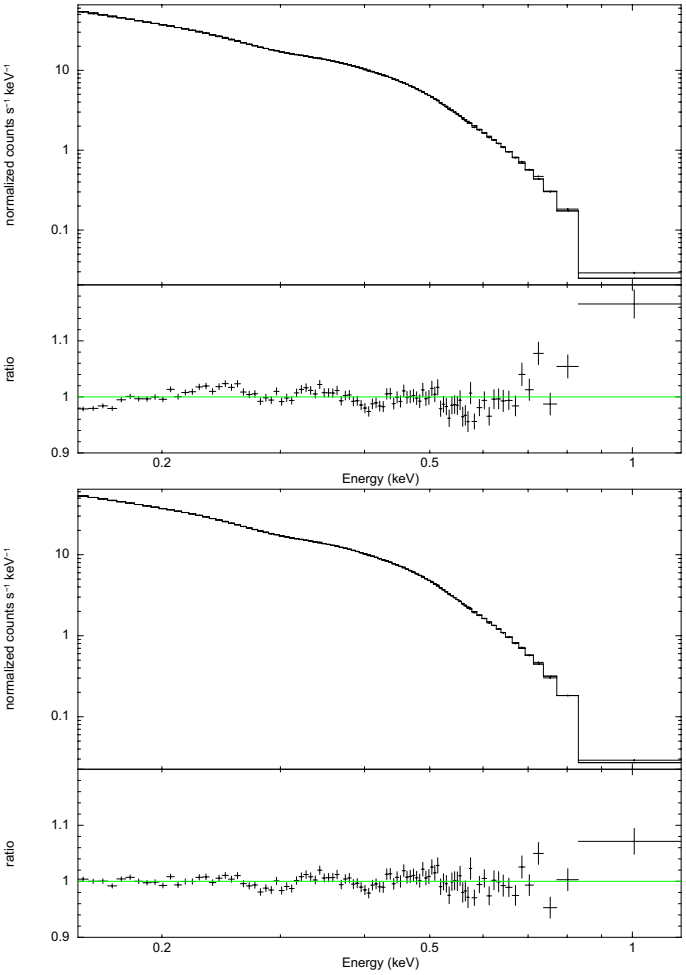

Fig. 5. (*Top*) Single BB fit of the merged spectrum obtained from observations of the "soft" group. (*Bottom*) Same as top panel but with a two BB model.

and *offset* of ∼4% and ∼15 eV, respectively, over the pn detector positions covered by the J1856 observations (Fig. 3).

Using only homogeneous data, we have found that the rate of temperature variations, in the framework of the single BB model, is compatible with a constant at 2σ confidence level over the past five years of the monitoring campaign. A higher temperature was recorded on April 2002. If not caused by subtle alterations to the instrument response, this difference would imply that J1856 also undergoes spectral changes, albeit the magnitude of these changes is much smaller than that observed for J0720. The

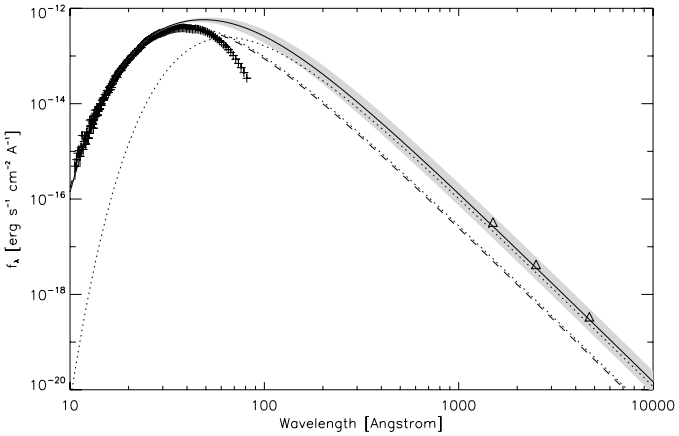

Fig. 6. Broad-band spectrum of J1856. The dashed line is the extrapolation of the (unabsorbed) X-ray BB from Burwitz et al. (2003). The dotted lines indicate the two BB components obtained from the sum of all the homogeneous observations with the source in the "soft" region, and the solid line is their sum. The shaded area marks the 1σ confidence region for the best-fit model. The triangles represent the optical/UV data obtained from HST photometry (Kaplan et al. 2011).

observed temperature changed by about 0.5 eV in three years (or less, considering the lack of coverage between April 2002 and March 2005) corresponding to a rate of ∼–0.15 eV yr^{-1}. In any case, the long-term behavior of J1856 differs markedly from that of J0720. The latter has underwent substantial and continuous changes in its observed spectral properties over the years. Apart from the slightly higher temperature recorded in April 2002, J1856 instead exhibits a steady behavior, with no spectral variations over the past five years.

By merging all the homogeneous data-sets, we have obtained a large quality spectrum with which we have tested the validity of single and two BB models and checked for the presence of features in the spectrum of J1856. Apart from some narrow features that are likely due to calibration issues and already reported in the literature (Haberl 2007), we have found no convincing evidence of broad or narrow absorption features. The absence of lines thus remains one of the distinctive properties of J1856 among XDINSs (see also Hohle et al. 2012). The two BB model returns a better fit to the data and is more physically justified by the observed pulsations. A second, cooler BB component was invoked by Pons et al. (2002) to explain the optical/UV data but its contribution to the X-ray flux was considered negligible because of the apparent lack of pulsations reported for J1856 at that time (Braje & Romani 2002; Burwitz et al. 2003; Trümper et al. 2004). This implied that there is an upper limit to the temperature of the cold BB, $kT_{\rm opt}^{\infty} < 33$ eV, which in turn yielded a lower limit to the stellar radius of $R^{\infty} = ((R_{\rm opt}^{\infty})^2 + (R_{\rm X}^{\infty})^2)^{1/2} > 16\,(d/120\,{\rm pc})$ km. An even larger value was found by Hambaryan et al. (2011) for RBS 1223 (1RXS J130848.6+212708), which is another XDINS. We note however that they assumed a condensed surface with a thin hydrogen atmosphere model to fit the spectrum of this neutron star. Thus, the measure of the radius resulting from the fit is larger than that obtained with a BB spectrum. From our analysis, we instead found a smaller radius, $R^{\infty} = ((R_{\rm s}^{\infty})^2 + (R_{\rm h}^{\infty})^2)^{1/2} = 12.7^{+4.6}_{-0.2}\,(d/120\,{\rm pc})$ km, which is consistent at the 1σ level with the lower limit reported by Trümper et al. Thus, our result allows for a wide range of radii and does not provide a tight constraint on the EOS. In any case, we stress that the inferred parameters of a second BB in the X-ray spectrum of J1856 must be taken

with caution. In addition to the statistical and systematic errors reported above, the normalization and thus the radius of soft BB component is affected by systematic uncertainties because of the poorly constrained energy redistribution below ~0.4 keV. Large systematic deviations are also expected because J1856 is one of the main calibration targets used to determine the instrumental energy response, hence the pn response matrix is currently tuned to reproduce a X-ray spectrum of J1856 that is not inconsistent with its optical/UV flux, when a double BB models is assumed. With the caveat of the aforementioned uncertainties, the extrapolation of the cold BB also accounts for a large fraction of the reported optical excess (e.g. Kaplan et al. 2011), avoiding the need for the more complex models that have been proposed to explain the observed optical/UV flux.

4. Conclusions

The results presented in this work have shown that the small amplitude variations in the spectral parameters of the isolated neutron star RX J1856.5-3754, obtained by fitting its spectrum with a single absorbed BB model, are due to a non-uniform energy response of the EPIC-pn camera. Once this instrumental effect is taken into account, the upper limits to the relative temperature and flux variations in the period March 2005 until the present are $\Delta kT^{\infty} < 0.5\%$ and $\Delta f_X < 3\%$, respectively. These can be taken as a measure of the source+instrument long-term stability. A higher temperature was observed in April 2002. If this were caused by an intrinsic change in the source spectral properties, it would imply that variations on timescales of years, similar to those observed in the other XDINS RX J0720.4-3125, might be a common feature of this class of sources.

Since these two sources are the brightest and most widely observed XDINSs, their continuous monitoring will help us to characterize the differences and similarities in their long-term behavior, hence provide insights into the physical conditions on their surfaces, such as the magnetic field and temperature distributions. In the case of J1856, the steady emission has allowed us to sum all the data taken with the source at the same position on the detector, in order to obtain a spectrum with large count statistics. The resulting spectrum is best-fitted by a two BB model, which is also more justifiable than a single BB by the observation of pulsations at X-ray energies. In addition, the extrapolation at optical wavelengths of the emission from the two BBs accounts for the excess reported in the literature. However, owing to the uncertainties in the calibration of the pn at low energies, the radius of the star is not well-constrained.

Finally, the results presented here suggest that J1856 is possibly the best choice of calibration source for instruments observing in the soft X-ray domain. Moreover, the EPIC-pn detector onboard *XMM-Newton* is extremely stable over a long time-span (see above) and so, after taking into account a subtle spatial dependence of its spectral response, it can be considered as a reference instrument for the study of long-term spectral variability of X-ray sources.

Acknowledgements. We thank the anonymous referee for useful comments that greatly improved the previous version of the manuscript. We also thank M. Guainazzi and K. Dennerl for carefully reading the manuscript and for helpful discussions and suggestions. The *XMM-Newton* project is an ESA Science Mission with instruments and contributions directly funded by ESA Member States and the USA (NASA). We acknowledge the support of ASI/INAF through grant I/009/10/0.

References

Anders, E., & Grevesse, N. 1989, Geochim. Cosmochim. Acta, 53, 197
Arnaud, K. A. 1996, Astronomical Data Analysis Software and Systems V, 101, 17
Braje, T. M., & Romani, R. W. 2002, ApJ, 580, 1043
Burwitz, V., Haberl, F., Neuhäuser, R., et al. 2003, A&A, 399, 1109
de Vries, C. P., Vink, J., Méndez, M., & Verbunt, F. 2004, A&A, 415, L31
Haberl, F. 2007, Ap&SS, 308, 181
Haberl, F., Turolla, R., de Vries, C. P., et al. 2006, A&A, 451, L17
Hambaryan, V., Suleimanov, V., Schwope, A. D., et al. 2011, A&A, 534, A74
Ho, W. C. G., Kaplan, D. L., Chang, P., van Adelsberg, M., & Potekhin, A. Y. 2007, MNRAS, 375, 821
Hohle, M. M., Haberl, F., Vink, J., et al. 2010, A&A, 521, A11
Hohle, M. M., Haberl, F., Vink, J., de Vries, C. P., & Neuhäuser, R. 2012, MNRAS, 419, 1525
Kaplan, D. L., & van Kerkwijk, M. H. 2005, ApJ, 628, L45
Kaplan, D. L., van Kerkwijk, M. H., & Anderson, J. 2007, ApJ, 660, 1428
Kaplan, D. L., Kamble, A., van Kerkwijk, M. H., & Ho, W. C. G. 2011, ApJ, 736, 117
Lai, D. 2001, Rev. Mod. Phys., 73, 629
Mereghetti, S. 2008, A&AR, 15, 225
Pons, J. A., Walter, F. M., Lattimer, J. M., et al. 2002, ApJ, 564, 981
Pons, J. A., Miralles, J. A., & Geppert, U. 2009, A&A, 496, 207
Read, A. M., Sembay, S. F., Abbey, T. F., & Turner, M. J. L. 2006, The X-ray Universe 2005, 604, 925
Strüder, L., Briel, U., Dennerl, K., et al. 2001, A&A, 365, L18
Stuhlinger, M., et al. 2011, Status of the *XMM-Newton* Cross-calibration with SASv10.0, `http://xmm2.esac.esa.int/docs/documents/CAL-TN-0052.ps.gz`
Tiengo, A., & Mereghetti, S. 2007, ApJ, 657, L101
Trümper, J. E., Burwitz, V., Haberl, F., & Zavlin, V. E. 2004, Nucl. Phys. B Proc. Supp., 132, 560
Turolla, R. 2009, Astrophys. Space Sci. Lib., 357, 141
Turolla, R., Zane, S., & Drake, J. J. 2004, ApJ, 603, 265
van Kerkwijk, M. H., & Kulkarni, S. R. 2001, A&A, 378, 986
van Kerkwijk, M. H., Kaplan, D. L., Pavlov, G. G., & Mori, K. 2007, ApJ, 659, L149
van Kerkwijk, M. H., & Kaplan, D. L. 2008, ApJ, 673, L163
Vink, J., de Vries, C. P., Méndez, M., & Verbunt, F. 2004, ApJ, 609, L75
Yakovlev, D. G., Ho, W. C. G., Shternin, P. S., Heinke, C. O., & Potekhin, A. Y. 2011, MNRAS, 411, 1977
Walter, F. M., & Lattimer, J. M. 2002, ApJ, 576, L145
Walter, F. M., Wolk, S. J., & Neuhäuser, R. 1996, Nature, 379, 233
Walter, F. M., Eisenbeiß, T., Lattimer, J. M., et al. 2010, ApJ, 724, 669